



Glucose Electrooxidation Study on 3-iodo-2-(aryl/alkyl)benzo[b]thiophene Organic Catalyst

Omruye Ozok-Arici¹ · Sefika Kaya² · Aykut Caglar^{1,3} · Hilal Kivrak^{2,4} · Arif Kivrak^{1,5} 

Received: 23 October 2021 / Accepted: 4 January 2022
© The Minerals, Metals & Materials Society 2022

Abstract

The compound 3-iodo-2-(aryl/alkyl)benzo[b]thiophene (4A-F) has been synthesized as an anode catalyst using the Sonogashira coupling reaction and the electrophilic cyclization reaction in moderate to excellent yields. The glucose electro-oxidation performance of these catalysts has been investigated by electrochemical methods, such as cyclic voltammetry (CV), chronoamperometry (CA), and electrochemical impedance spectroscopy (EIS) in 1 M KOH + 1 M C₆H₁₂O₆ solution. When Pd metal is electrochemically deposited on the organic catalyst to increase the electrocatalytic activities, the Pd@4A catalyst exhibits the highest catalytic activity with 0.527 mA/cm² current density than the 4A. The CA and EIS results prove that the Pd@4A catalyst has long-term stability and low charge transfer resistance and may be used in metal–organic catalyst systems as an anode catalyst to improve their performance. The results confirm that benzothiophene-based metal systems will be environmentally friendly materials in glucose fuel cells.

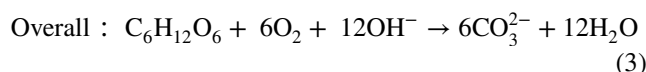
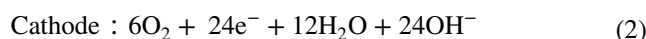
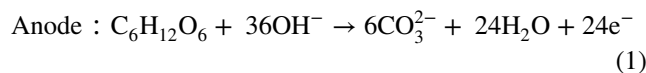
Keywords Palladium · glucose electro-oxidation · benzothiophene · energy

Introduction

Non-renewable fossil fuels (coal, oil and natural gas) have been main energy sources all over the world for the last century.¹ With increasing world population and industrialization, energy has gained great importance.^{2–4} It is known that fossil fuels increase gas emissions, leading to climate change.^{5,6} In

2020, the Intergovernmental Panel on Climate Change published comprehensive reports based on scientific, technical, and socio-economic assessments. According to these reports, climate change will become a major problem for the future, with increasing risks throughout the world. Therefore, clean energy sources are urgently required. Fuel cells are promising as a sustainable and efficient energy source for a clean future.^{7–11}

Glucose is an important simple sugar that is abundant in nature. It has a high energy density and is a potential hydrogen carrier. Moreover, it is used as a fuel in direct liquid fuel cells with its advantages of easy usability, as well as being non-volatile, non-toxic, non-explosive, and cheap.^{12–14} A glucose molecule can produce 24 e⁻ and yield – 2870 kJ/mol of energy via the complete oxidation to CO₂.¹⁵ Glucose electro-oxidation reactions in alkaline media are as follows:



The slow oxidation kinetics of glucose and the intermediate products formed during oxidation cause poisoning of

✉ Hilal Kivrak
hilalkivrak@gmail.com; hilaldemir.kivrak@ogu.edu.tr

✉ Arif Kivrak
arif.kivrak@ogu.edu.tr

¹ Technology and Innovation Center, Advance Organic Synthesis Laboratory, Eskisehir Osmangazi University, Eskişehir 26040, Turkey

² Department of Chemical Engineering, Faculty of Engineering and Architectural Sciences, Eskisehir Osmangazi University, Eskisehir 26040, Turkey

³ Department of Chemical Engineering, Faculty of Engineering, Van Yüzüncü Yil University, Van 65000, Turkey

⁴ Translational Medicine Research and Clinical Center, Eskisehir Osmangazi University, 26040 Eskisehir, Turkey

⁵ Faculty of Sciences and Arts, Department of Chemistry, Eskisehir Osmangazi University, Eskişehir 26040, Turkey

the anode catalyst in direct glucose fuel cells (DGFC).^{16,17} Many electrocatalysts have been developed by researchers to remove these barriers of DGFC. Basu et al. synthesized bimetallic (PdPt/C) and trimetallic (PtPdAu/C) catalysts by NaBH₄ reduction as anode catalysts for glucose electro-oxidation. They reported that the trimetallic catalyst exhibited more stable electroactivity in DGFC with 0.52 mW/cm² power density.¹⁸ Brouzgou et al. studied Pd/C, PdSn/C, and Pd₃Sn₂/C anode catalysts in an alkaline medium. They investigated the effects of electrolyte and glucose concentration on glucose oxidation. They stated that electro-oxidation activity increased with increasing glucose concentration.¹⁹ Nickel–cobalt composite materials supported by activated carbon were synthesized by Gao et al. for glucose oxidation. They reported that the power density reached 2.40 mW/cm² with the synergistic effect of the Ni-Co composite used as the anode catalyst.²⁰ Likewise, many different materials, such as G-ITO,²¹ PdRh/C,²² Au/GO,²³ NiCrCo,²⁴ Pd₃Au₇/C,²⁵ C-TNT,²⁶ Pd-Bi/C,²⁷ AuAg/C,²⁸ and Pd-Rh/CNT,²⁹ have been investigated as anode catalysts in DGFC to increase the electro-activity of glucose oxidation.

A variety of heterocyclic compounds have been used in medicinal and material applications, and are also very important for the synthesis of organic compounds due to their useful properties.³⁰ Recently, we investigated a fuel cell anode catalyst by using hetero-aromatic compounds like benzothiophenes and indoles.^{31,32} Benzothiophenes possess exciting biological properties, and are unique pharmacophores of several bioactive molecules.³³ Moreover, they have high stability, high conductivity, and can easily undergo reactions for the formation of active molecules.^{34,35}

In the light of the previous studies,^{36–38} 3-iodo-benzothiophene derivatives were synthesized via coupling reactions and electrophilic cyclization reactions. After characterization, the glucose electro-oxidation activities of these organic catalysts as anode catalysts were investigated. In addition, Pd metal was electrodeposited onto the benzothiophene derivatives to discover the effects of electrochemical activity. A Pd-doped organic catalyst (Pd-4A) was characterized by using electron microscopy with energy dispersive x-ray (SEM-EDX) and transmission electron microscopy (TEM). Pd-Organic catalyst systems can be important to study as fuel cell anode catalysts.

Experimental

Preparation of Organic Catalysts

Synthesis of (2-((aryl/alkyl)ethynyl)phenyl)(methyl)sulfane (3A)

2-Iodothianisole (1) (1 equiv.), PdCl₂(PPh₃)₂ (0.05 equiv.), 1-ethynyl-4-methoxybenzene (2) (1.2 equiv.) and CuI (0.05

equiv.) in THF (10 mL) and triethylamine (15 mL) were mixed at room temperature overnight. When the starting compound was used up, the mixture was extracted with EtOAc (3 × 15 mL). The combine organic phase was dried with anhydrous MgSO₄, filtered, and then concentrated under reduced pressure. The residue was purified by using flash column chromatography on silica gel hexane/ethyl acetate (100:1) to give (2-((aryl/alkyl)ethynyl)phenyl)(methyl)sulfane (3A-F).³⁸

General Procedure for Synthesis of 3-iodo-2-(aryl)benzo[b]thiophene (4A-F)

(2-((4-Methoxyphenyl)ethynyl)phenyl)(methyl)sulfane (3A) (1 equiv.) in dichloromethane (30 mL) was added to molecular iodide (2 equiv.) at room temperature. After 3 h, the reaction mixture was washed with saturated Na₂S₂O₃ and extracted with dichloromethane (3 × 20 mL). The combine organic phase was dried with anhydrous MgSO₄, filtered, and then concentrated under reduced pressure. The residue was purified by using flash column chromatography on silica gel hexane/ethyl acetate (100:1) to give 3-iodo-2-(aryl/alkyl)benzo[b]thiophene (4A-F).

Electrochemical Measurements

Electrochemical measurements were implemented employing the CHI 660E potentiostat device to determine the glucose electro-oxidation activities of the catalysts. Cyclic voltammetry (CV), chronoamperometry (CA), and electrochemical impedance spectroscopy (EIS) measurements were performed in a three-electrode system consisting of glassy carbon electrode (working electrode), Pt wire (counter electrode), and Ag/AgCl (reference electrode) in 1 M KOH + 1 M C₆H₁₂O₆ solution. The effects of the scan rate and KOH and glucose concentrations on the glucose electro-oxidation were also investigated. The electro-oxidation activities of the catalysts were determined via CV at 50 mV/s in the potential range of – 0.6 V–0.8 V. The Pd was electrochemically deposited on the organic catalyst electrode by CV in 0.002 mmol K₂PdCl₄ + 2.0 mmol H₂SO₄ + 0.004 mmol HCl solution at 10 mV/s scan rate.³⁹ Pd electrodeposition on glassy carbon modified with the organic catalyst was continued during 20 cycles by CV analysis. Afterward, electrochemical analyses were realized with this electrode. CA measurements for the stability of Pd@4A catalyst were performed at – 0.4V, – 0.2V, 0.0V, 0.2V, and 0.4 V potentials for 1000 s. The electrochemical resistance of this catalyst was investigated by EIS at 316 kHz to 0.046 Hz frequency and 5 mV amplitude.

Results and Discussion

Synthesis

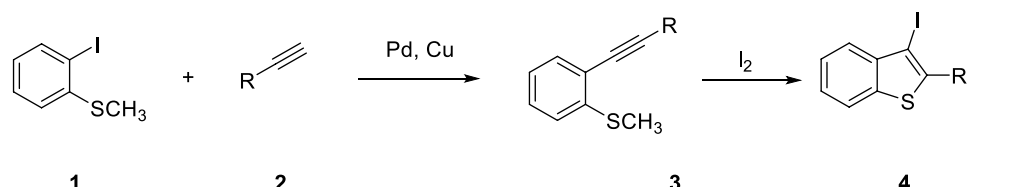
Initially, the Sonogashira coupling reaction was applied for the formation of 2-((4-methoxyphenyl)ethynyl)phenyl (methyl)sulfane (3A). When 2-iodothianisole 1 was allowed to react with 1-ethynyl-4-methoxybenzene 2 in the presence of a Pd/Cu catalyst at room temperature under an inert atmosphere, the intermediate 3A was isolated in 88% yields. By using the same reaction conditions, six benzothiophene derivatives (4B-F) were synthesized with between 72% and 95% yields (Table I). Recent studies have proved that electrophilic cyclization reactions (ECRs) can be more useful synthetic methods for the formation of halogene-substituted heterocyclic compounds. ECRs have many advantages, such as the high yields, high regioselectivity, and the need for cheaper and environmentally friendly catalysts like molecular iodide. In the present study, 3-iodo-2-(4-methoxyphenyl)benzo[b]thiophene A was obtained by using ECRs (76% yield) (Table I). When heptyne was used as the starting alkyne, compound 4B was isolated in 95% yields. To find the substituent effects of electro-oxidation, a variety of benzothiophenes, including aromatic and polyaromatics, were prepared with moderate to high yields (Table I).

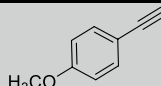
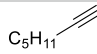
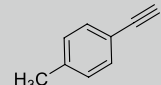
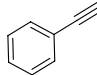
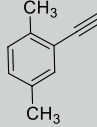
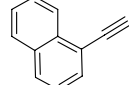
Characterization Results

SEM-EDS and mapping analysis were employed to examine the surface morphology of the Pd@4A catalyst, and the results are shown in Fig. 1a–h. Since the catalyst contains a low amount of metal, the metal atoms may not be visible in the SEM images (Fig. 1a, b). However, as seen in the EDS and mapping results (Fig. 1c–h), Pd, O, C, and N were obtained on the catalyst surface. According to the results of the analysis made from just one point (Fig. 1c), these were determined as O (d) turquoise, N (e) yellow, Pd (f) red, and C (g) blue colors. In addition, the presence of Pd metal atoms by EDS analysis shows that it is electrochemically deposited on the organic material.

The morphology and structure of the d@4A catalyst were examined via TEM analysis, and Fig. 2a–f shows the TEM images and histograms of the catalyst. The TEM images indicate that Pd particles are formed without agglomeration at certain points. The histograms of the 20-nm and 50-nm images were obtained utilizing the ImageJ program. The particle size was calculated as being an average 2 nm. Although it is not clear in the SEM analysis due to the small particle size, the Pd particles were successfully deposited on the organic material surface, as shown in the EDS and mapping results. In addition, it has been emphasized in many studies

Table I Synthesis of 3-iodo-2-arylbenzothiophene derivatives



Entry	Alkyne 2	Intermediate 3 (Yield) ^a	Benzothiophene 4 (Yield) ^a
1		3A (88%)	4A (76%)
2		3B (94%)	4B (95%)
3		3C (88%)	4C (78%)
4		3D (92%)	4D (86%)
5		3E (88%)	4E (72%)
6		3F (72%)	4F (75%)

^a Isolated yields.

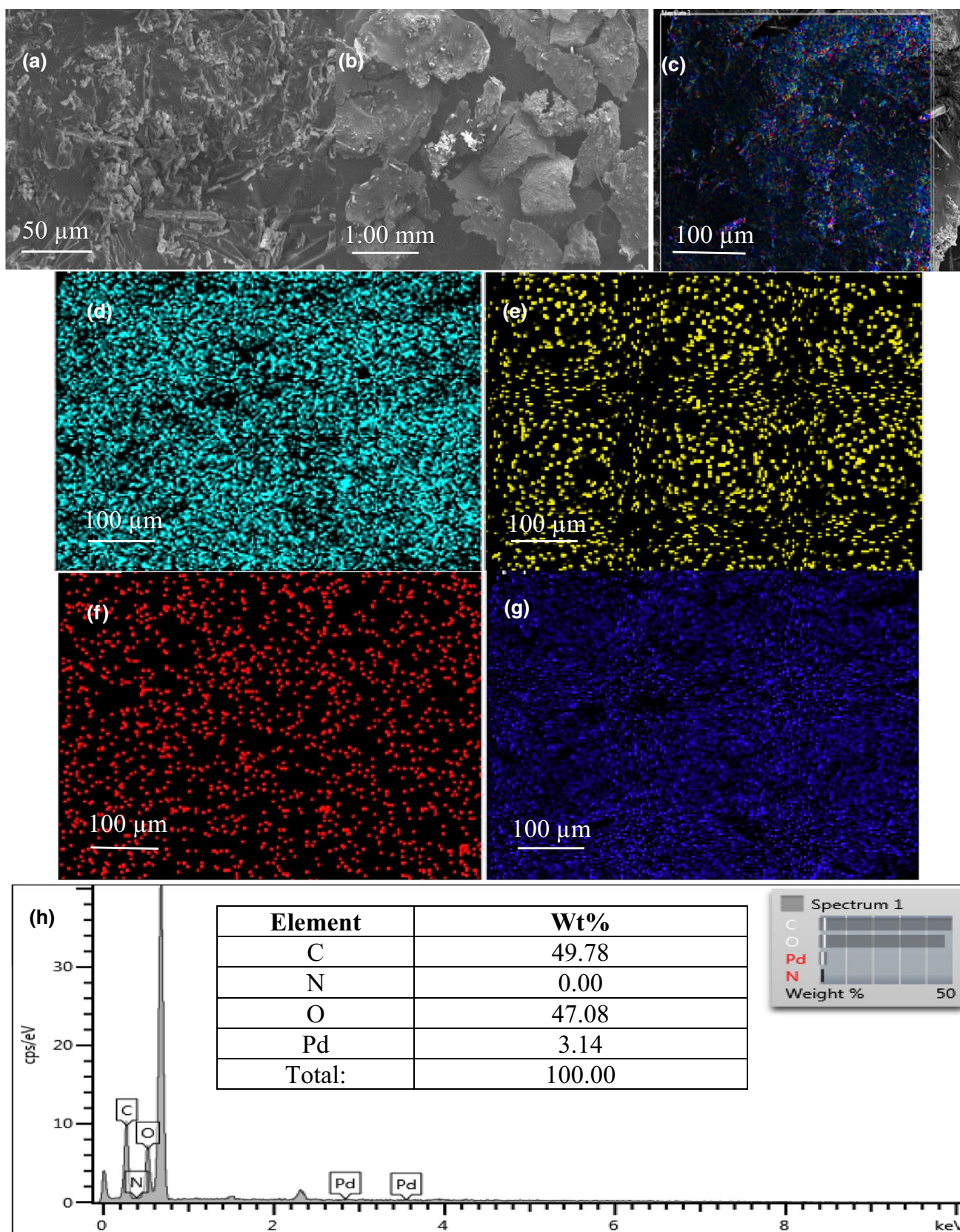


Fig. 1 SEM-EDX (a, b, h) and mapping images: mapping and EDX point (c), O (d), N (e), Pd (f), C (g) of the Pd-4A catalyst.

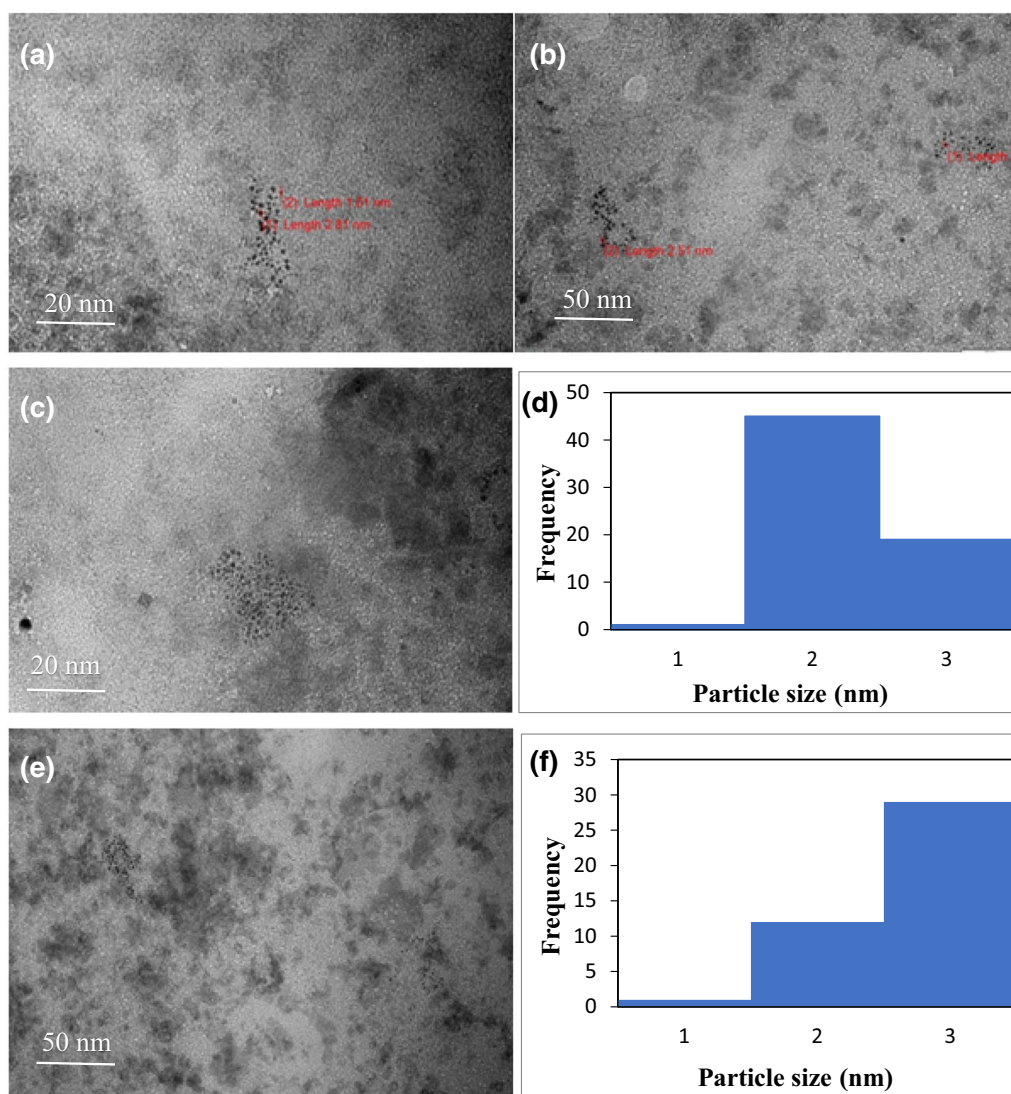


Fig. 2 TEM images of (a, c) 20 nm and (b, e) 50 nm with the related particle size distribution (d, f) for the Pd@4A catalyst.

in the literature that the catalytic activity increases as the particle size decreases.^{40,41}

Electrochemical Results

The glucose electro-oxidation activities of organic catalysts were investigated by CV measurements in 1 M KOH + 1 M C₆H₁₂O₆ solution. CV voltammograms of the catalysts in the potential range of -0.6–0.8 V are presented in Fig. 3. No oxidation peaks were observed in the glucose

electro-oxidation results of the organic catalysts. Therefore, the results have been interpreted over the total current. The current values of the organic catalysts are given in Table II. The 4E organic catalyst displayed the highest catalytic performance, at 0.025 mA/cm². The Pd were deposited with 20 cycles on the organic catalysts to increase the electrochemical activity. Figure 4 shows CV voltammograms of Pd-doped organic catalysts. The oxidation peaks were observed in the forward scan direction of the catalysts. These peaks indicate electro-oxidation from glucose adsorption.^{7,29} The Pd@4A catalyst performed better than other organic catalysts in

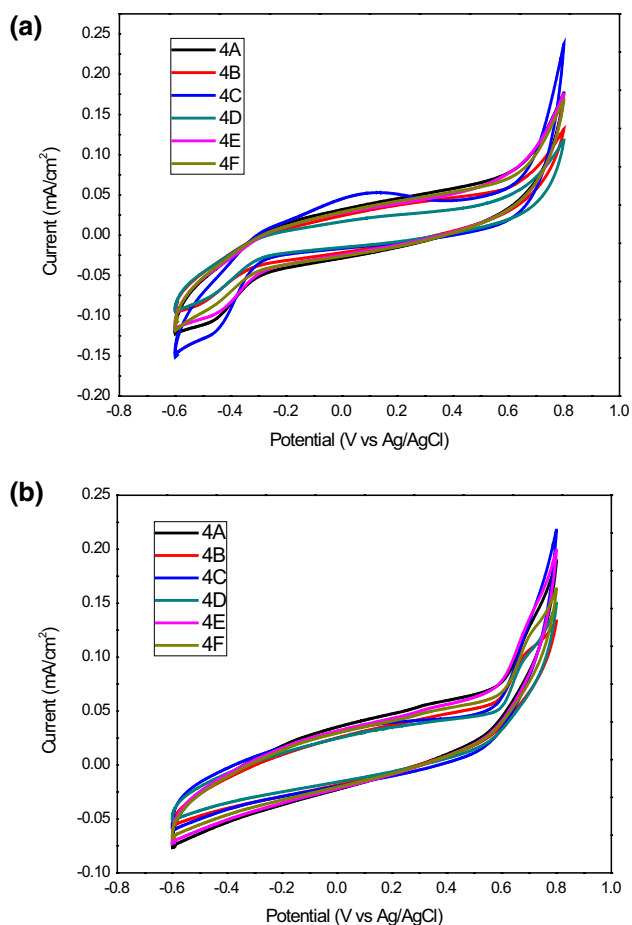


Fig. 3 Cyclic voltammograms of organic catalysts in (a) 1 M KOH and (b) 1 M KOH + 1 M $C_6H_{12}O_6$ solution (scan rate 50 mV/s).

Table II Electrochemical properties of organic catalysts for glucose electro-oxidation

Catalyst	Total current of KOH, mA/cm ²	Total current of $C_6H_{12}O_6$, mA/cm ²	Normal current, mA/cm ²
4A	0.172	0.188	0.016
4B	0.131	0.133	0.002
4C	0.233	0.216	-0.020
4D	0.118	0.149	0.031
4E	0.173	0.198	0.025
4F	0.166	0.163	-0.003

glucose electro-oxidation. When Pd was doped on the 4A organic catalyst, its specific activity increased and reached 0.527 mA/cm^2 . Next, CV results obtained by doped Pd on the 4A catalyst in different cycles are presented in Fig. 5. Table III includes the specific activities, onset (E_{on}) and peak (E_p) potentials of the Pd-doped organic catalysts.

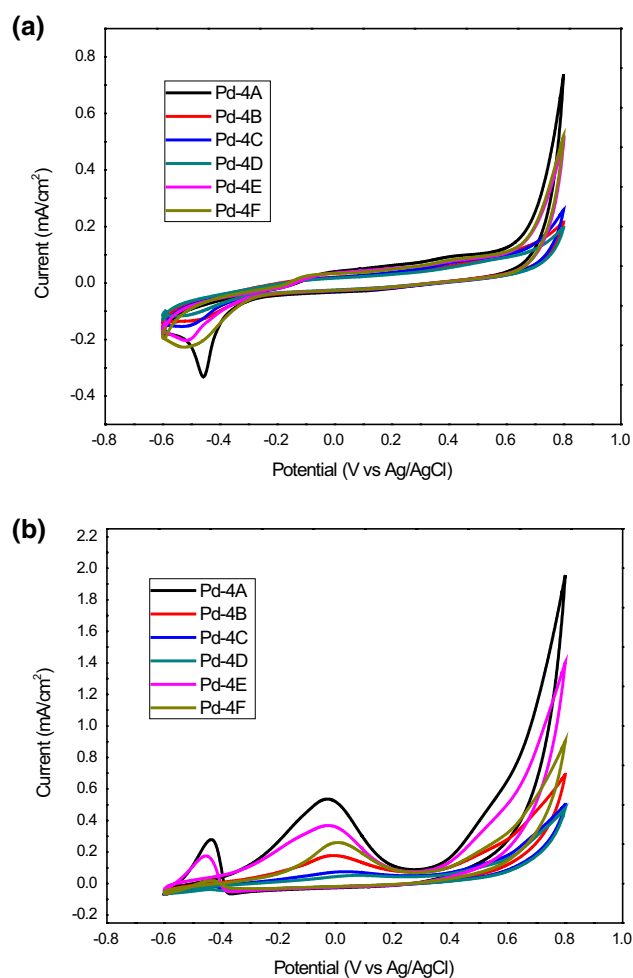


Fig. 4 Cyclic voltammograms of Pd-doped organic catalysts in (a) 1 M KOH and (b) 1 M KOH + 1 M $C_6H_{12}O_6$ solution (scan rate 50 mV/s).

The electrocatalytic activities of the catalysts were greatly increased by depositing Pd.

The effect of scanning rate, glucose concentration, and KOH concentration change of Pd@4A on glucose electro-oxidation were researched and the results are represented in Fig. 6. The highest activity was reached at 100 mV/s in experiments performed at different scanning rates ranging from 1 mV/s to 100 mV/s. The glucose electro-oxidation activity of Pd@4A was investigated by keeping the KOH concentration constant at 1 M and changing the glucose concentrations in the range of 0.0025 M–2 M. The highest catalytic activity was achieved at 0.1 M glucose concentration. In the study of the effect of KOH concentration on glucose electro-oxidation, the glucose concentration was kept constant as 0.1 M and the KOH concentrations were changed in the same range. The highest catalytic activity was attained at 2 M KOH concentration.

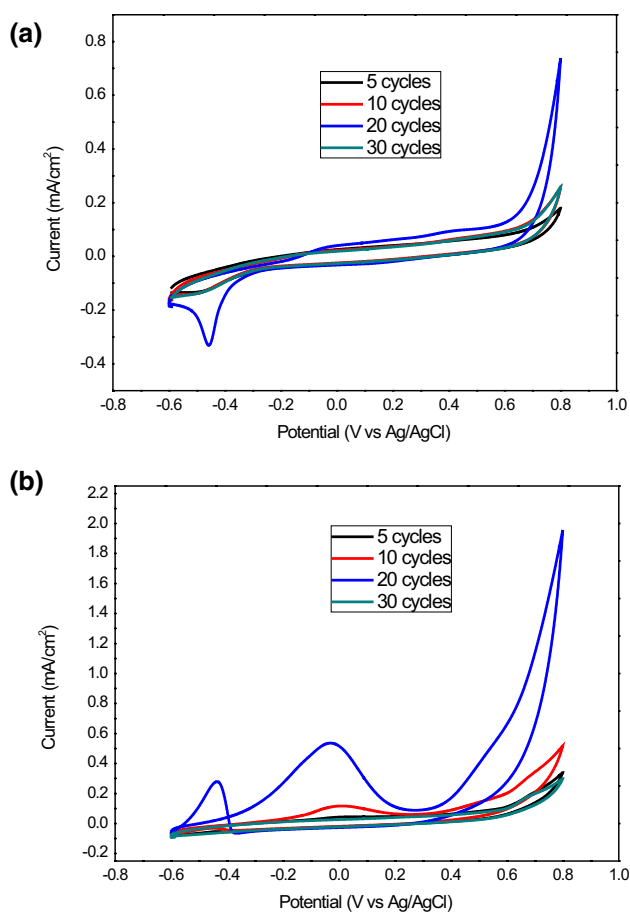


Fig. 5 Cyclic voltammograms of 4A doped with Pd at different cycles in (a) 1 M KOH and (b) 1 M KOH + 1 M $C_6H_{12}O_6$ solution (scan rate 50 mV/s).

Table III Electrochemical properties of Pd-doped organic catalysts for glucose electro-oxidation

Catalyst	Specific activity, mA/ cm^2	E_p , V	E_{on} , V
Pd@4A	0.527	-0.04	-0.52
Pd@4B	0.180	-0.01	-0.57
Pd@4C	0.078	0.025	-0.58
Pd@4D	0.053	0.06	-0.57
Pd@4E	0.370	-0.03	-0.50
Pd@4F	0.261	0.01	-0.49

In order to determine the stability of the Pd@4A catalyst, CA measurements were taken at -0.4 V, -0.2 V, 0, 0.2 V, and 0.4 V potentials for 1000 s, and the CA curves are shown in Fig. 7. An initial rapid current density drop followed by a slow current density drop was observed at all potentials. This rapid initial decline can be explained by the poisoning of the electrode surface by intermediate species

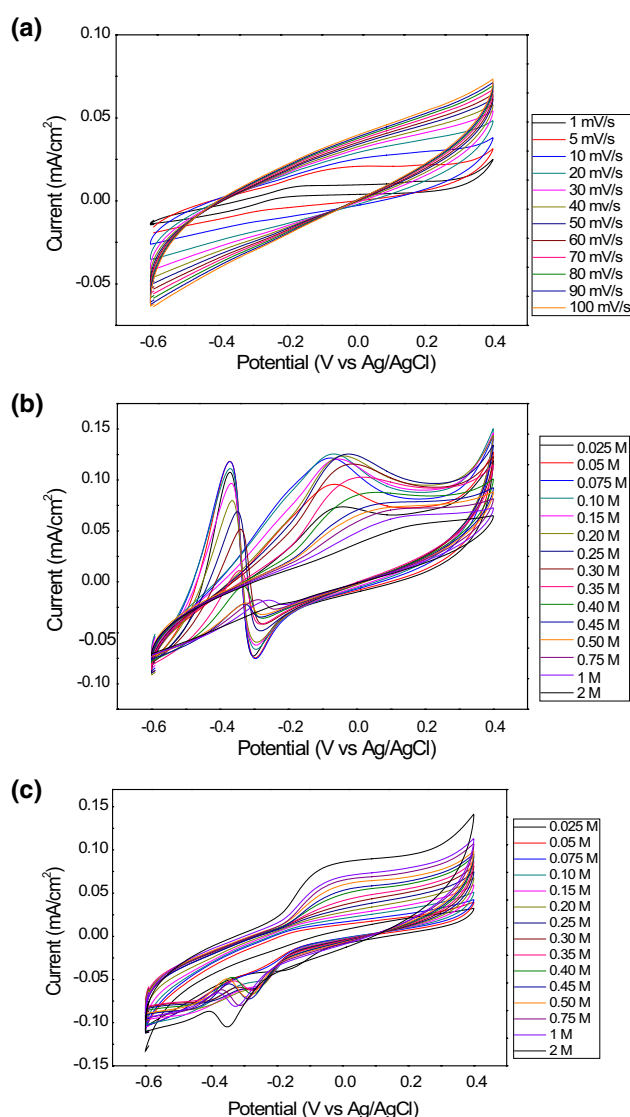


Fig. 6 Cyclic voltammograms of Pd@4A catalyst for (a) different scan rates, (b) different glucose concentrations, (c) different KOH concentrations.

formed during electro-oxidation. The longest and highest stability of the Pd-doped organic catalyst was obtained at 0.4 V potential. Then, it was compared with the organic catalyst at a potential of 0.4 V, from which it can be seen that the current stability of the Pd-doped organic catalyst was higher than the organic catalyst.

Nyquist curves from the EIS results were used to determine the resistance to glucose electro-oxidation. In the Nyquist diagrams, as the diameter of the semicircle decreases, the charge transfer resistance decreases, and therefore the electrocatalytic activity increases.⁴² Lower charge transfer resistance (R_{ct}) means a larger electroactive surface area and faster electron transfer rate between the electrolyte and the electrode.⁴³ EIS measurements were performed at different potentials of -0.6V, -0.4V, -0.2V, 0, 0.2V, and 0.4 V. As seen in Fig. 8,

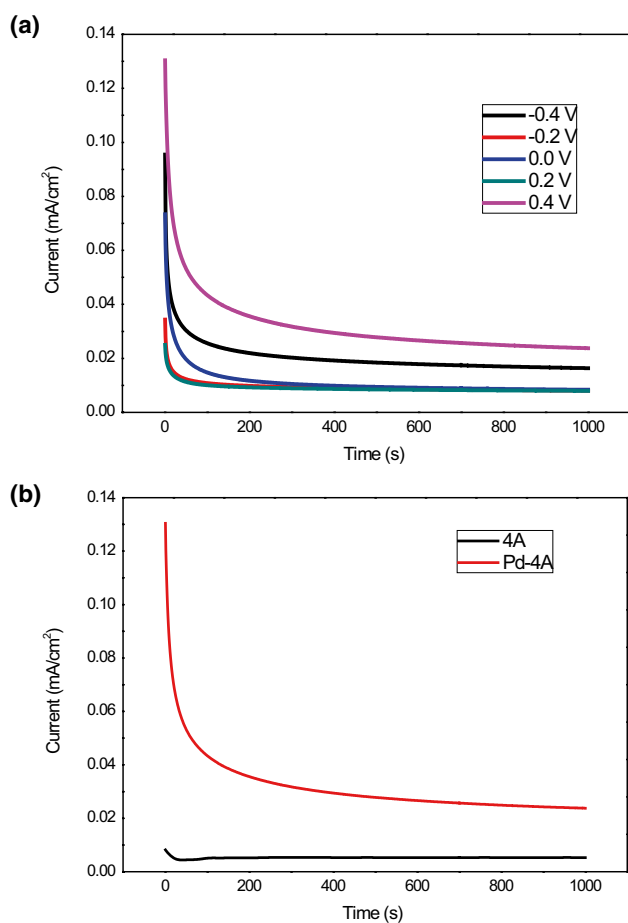


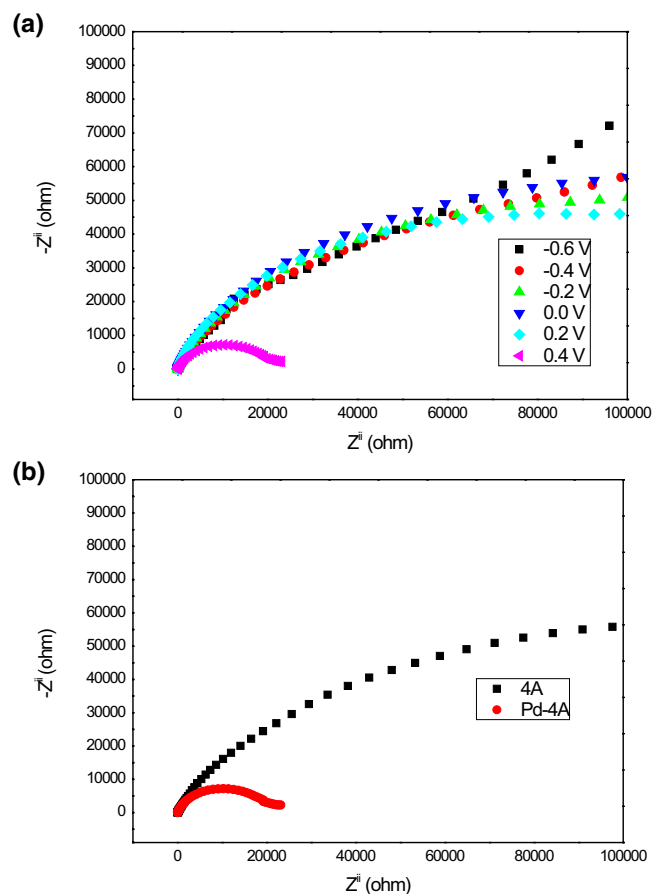
Fig. 7 Chronoamperograms of (a) Pd@4A catalyst at different voltages, (b) comparison with organic catalyst at 0.4 V and 1000 s.

the impedance behavior of the Pd-doped organic catalyst changed as the applied potential changed. The lowest charge transfer resistance was reached at a potential of 0.4 V. This result was consistent with the results from CA.

Conclusions

The compound 3-iodo-2-(aryl/alkyl)benzo[b]thiophene (A-F) was synthesized via Pd-catalyzed Sonogashira cross-coupling reaction and electrophilic cyclization reaction. The isolated yields of the desired products changed between 72% and 95% yields. Their performance was investigated as anode catalysts for glucose electro-oxidation. Surprisingly, when benzothiophene derivatives were electrodeposited with Pd metal, the glucose electro-oxidation activities of Pd depositing on the organic catalysts increased. The highest catalyst performance was observed for the Pd@4A catalyst system at 0.527 mA/cm² current density with high stability and low charge transfer resistance. The Pd@4A catalyst is characterized by advanced surface characterization techniques, such as SEM-EDX and TEM. The characterization results confirmed the successful deposition of Pd particles on the catalyst. As a result, our catalyst has significant properties such as cheaper than metal catalysts and more environmentally friendly than metals. Pd@benzothiophene catalyst systems may be worth further study as an anode catalyst in glucose electro-oxidation.

Fig. 8 Nyquist plots of (a) Pd@4A at different voltages, (b) comparison with organic catalyst at 0.4 V.



Acknowledgments The authors thank to Eskişehir Osmangazi University BAP (Project No: FOA-2021-2203) for chemicals and solvents. The author (A. Kivrak) would like to acknowledge networking contribution by the COST Action CA17104 “New diagnostic and therapeutic tools against multidrug resistant tumours”.

Conflict of interest All authors declare that there is no conflict of interest.

References

- S.A. Asongu, M.O. Agboola, A.A. Alola, and F.V. Bekun, *Sci. Total Environ.* 712, 136376 (2020).
- J. Liu, C. Chen, Z.L. Liu, K. Jermstiparsert, and N. Ghadimi, *J. Energy Storage.* 27, 101057 (2020).
- W.B. Huang, and M. Marefati, *Energy Rep.* 6, 2919 (2020).
- B. Ulas, A. Caglar, A. Kivrak, and H. Kivrak, *Chem. Pap.* 73, 425 (2019).
- D.Z. Li, J.A. Guo, J. Zhang, L.N. Zhan, and M. Alizadeh, *J. Energy Storage.* 39, 102631 (2021).
- A. Caglar, D. Duzenli, I. Onal, I. Tezsevin, O. Sahini, and H. Kivrak, *J. Phys. Chem. Solids.* 150, 109684 (2021).
- A. Caglar, B. Ulas, O. Sahin, and H. Kivrak, *Int. J. Energy Res.* 43, 8204 (2019).
- M.Y.P. Peng, C.C. Chen, X.H. Peng, and M. Marefati, *Sustain. Energy Technol. Assess.* 39, 100713 (2020).
- Z.F. Pan, L. An, T.S. Zhao, and Z.K. Tang, *Prog. Energy Combust. Sci.* 66, 141 (2018).
- M. Marefati, M. Mehrpooya, and M.B. Shafii, *Energy Convers. Manag.* 183, 193 (2019).
- H. Kivrak, D. Atbas, O. Alal, M.S. Cogenli, A. Bayrakceken, S.O. Mert, and O. Sahin, *Int. J. Hydrog. Energy.* 43, 21886 (2018).
- Y. Zhao, X.H. Liu, X. Wang, P.P. Zhang, and J.F. Shi, *Int. J. Hydrog. Energy.* 42, 29863 (2017).
- M.Q. Hao, X.H. Liu, M.N. Feng, P.P. Zhang, and G.Y. Wang, *J. Power Sources.* 251, 222 (2014).
- L. Yang, X.H. Liu, J. Ding, S.L. Li, F. Dong, M. Irfan, Y. Li, G.Y. Wang, X.W. Du, and P.P. Zhang, *Int. J. Hydrog. Energy.* 44, 2823 (2019).
- Y.L. Yang, X.H. Liu, M.Q. Hao, and P.P. Zhang, *Int. J. Hydrog. Energy.* 40, 10979 (2015).
- D. Basu, and S. Basu, *Electrochim. Acta.* 55, 5775 (2010).
- J.Y. Chen, C.X. Zhao, M.M. Zhi, K.W. Wang, L.L. Deng, and G. Xu, *Electrochim. Acta.* 66, 133 (2012).
- D. Basu, and S. Basu, *Int. J. Hydrog. Energy.* 37, 4678 (2012).
- A. Brouzgou, S. Song, and P. Tsiakaras, *Appl. Catal. B* 158, 209 (2014).
- M.Y. Gao, X.H. Liu, M. Irfan, J.F. Shi, X. Wang, and P.P. Zhang, *Int. J. Hydrog. Energy.* 43, 1805 (2018).
- A. Caglar, B. Ulas, O. Sahin, and H.D. Kivrak, *Energy Storage.* 1, 4 (2019).
- A. Brouzgou, L.L. Yan, S.Q. Song, and P. Tsiakaras, *Appl. Catal. B* 147, 481 (2014).

23. R.A. Escalona-Villalpando, M.P. Gurrola, G. Trejo, M. Guerra-Balcazar, J. Ledesma-Garcia, and L.G. Arriaga, *J. Electroanal. Chem.* 816, 92 (2018).
24. Y.Y. Gu, H.H. Yang, B.Q. Li, and Y. An, *Electrochim. Acta.* 192, 296 (2016).
25. T. Rifaideen, S. Baranton, and C. Coutanceau, *Appl. Catal. B* 243, 641 (2019).
26. A. Caglar, H. Kivrak, N. Aktas, and A.O. Solak, *J. Electron. Mater.* 50, 2242 (2021).
27. C.C. Chen, C.L. Lin, and L.C. Chen, *J. Power Sources.* 287, 323 (2015).
28. F.M. Cuevas-Muniz, M. Guerra-Balcazar, F. Castaneda, J. Ledesma-Garcia, and L.G. Arriaga, *J. Power Sources.* 196, 5853 (2011).
29. C.T. Hsieh, Y.F. Chen, and P.Y. Yu, *Int. J. Hydrog. Energy.* 40, 14857 (2015).
30. R.D. Taylor, M. MacCoss, and A.D.G. Lawson, *J. Med. Chem.* 57, 5845 (2014).
31. O. Ozok, E. Kavak, O.F. Er, H. Kivrak, and A. Kivrak, *Int. J. Hydrog. Energy.* 45, 28706 (2020).
32. A. R. Hamad, H. Calis, A. Caglar, H. Kivrak, and A. Kivrak, *Int. J. Energy Res.* 46, 1659 (2022).
33. R.S. Keri, K. Chand, S. Budagumpi, S.B. Somappa, S.A. Patil, and B.M. Nagaraja, *Eur. J. Med. Chem.* 138, 1002 (2017).
34. M.E. Cinar, and T. Ozturk, *Chem. Rev.* 115, 3036 (2015).
35. M. Guler, V. Turkoglu, and A. Kivrak, *Int. J. Biol. Macromol.* 79, 262 (2015).
36. M. A. S. Algso, A. Kivrak, M. Konus, C. Yilmaz, and A. Kurt-Kizildogan, *Int. J. Chem. Sc.* 130, 119 (2018).
37. M.A.S. Algso, and A. Kivrak, *Chem. Pap.* 73, 977 (2019).
38. O. Ozok, E. Kavak, and A. Kivrak, *Nat. Prod. Res.* (2021). <https://doi.org/10.1080/14786419.2021.1928116>
39. A. Caglar, D. Duzenli, I. Onal, I. Tersevin, O. Sahin, and H. Kivrak, *Int. J. Hydrog. Energy.* 45, 490 (2020).
40. D.S. Kim, S.J. Han, and S.Y. Kwak, *J. Colloid Interface Sci.* 316, 85 (2007).
41. C.H. Jiang, M.D. Wei, Z.M. Qi, T. Kudo, I. Honma, and H.S. Zhou, *J. Power Sources.* 166, 239 (2007).
42. W.L. Qu, Z.B. Wang, X.L. Sui, and D.M. Gu, *Int. J. Hydrog. Energy.* 39, 5678 (2014).
43. L. Karupphasamy, C.Y. Chen, S. Anandan, and J.J. Wu, *Catal. Today.* 307, 308 (2018).

Publisher's Note Springer Nature remains neutral with regard to jurisdictional claims in published maps and institutional affiliations.